IPPI

Polyolefins Journal, Vol. 3 No. 1 (2016) 23-36

ORIGINAL PAPER

Phillips catalysts synthesized over various silica supports: Characterization and their catalytic evaluation in ethylene polymerization

Ebrahim Ahmadi[1*], Zahra Mohamadnia[2*], Sajjad Rahimi[3], Mohammad Hasan Armanmehr[4], Mohammad Hossein Heydari[1], Mahmood Razmjoo[1]

[1] Department of chemistry, University of Zanjan, P.O. Box 45195-313, Zanjan, Iran
[2] Department of chemistry, Institute for Advanced Studies in Basic Sciences (IASBS), Gava zang, P. O. Box 45195-1159, Zanjan, Iran
[3] Department of Chemistry, College of Sciences, Shiraz University, Shiraz 71454, Iran
[4] Department of Chemical Technologies, Iranian Research Organization for Science and Technology, P.O. Box 15815-3538, Tehran, Iran

Received: 29 May 2015, Accepted: 7 September 2015

ABSTRACT

Ethylene polymerization was carried out using Phillips chromium catalyst based on silica supports such as silica aerogel, SiO_2 (Grace 643), and titanium modified SiO_2 (G 643), and the results were compared with other catalysts based on SiO_2 (Aldrich), SBA-15(Hex), SBA-15(Sp) and MCM-41. A combination of TGA, DSC, XRD, nitrogen adsorption, SEM, ICP, FTIR and other analyses were used to characterize the materials. The results showed that the chromium was successfully introduced into silica supports. Shish-kebab polyethylene was prepared via in situ ethylene polymerization with the Cr/SiO_2 (G 643) and $Cr/Ti/SiO_2$ (G 643) catalytic systems. A comparison between different types of catalysts revealed that the polymerization activity of Cr/SiO_2 (G 643) was significantly increased to 191 kg PE $(g\ Cr)^{-1}\ h^{-1}$ due to the higher pore volume and pore diameter of Grace silica compared to the other supports. Also, the polymerization activity of the Cr/SiO_2 (G 643) catalyst was significantly improved by Ti-modification. **Polyolefins J 3:23-36**

Keywords: Silica aerogel; Grace silica; chromium catalyst; ethylene polymerization; shish-kebab

INTRODUCTION

Phillips $CrOx/SiO_2$ catalysts, with highly dispersed chromium oxide covalently attached to a silica surface, are among the most widely used industrial polyethylene catalysts since discovered by Hogan and Banks in the early 1950s [1-3]. These well-known catalysts, nowadays produce about 10 million tons of high-density polyethylene (HDPE) annually, which correspond to about 50% of the world HDPE production [4]. Compared with the other polyolefin catalysts, such as Ziegler–Natta and metallocene catalysts, the Phillips catalyst shows distinctive polymerization behaviors and can produce HDPE with ultra-broad molecular weight distribution (MWD) and chain branches including short and long chain branches, which contribute some unique characteristics for commercial applications like blow-molding HDPE production [5,6]. Despite the numerous research efforts during the past 60 years, the academic progresses on this catalyst are lagging far behind its successful commercial applications [7].

Generally, the Phillips catalyst consists of hexavalent chromium supported on a high-surface-area, wide-pore oxide carrier, such as silica, alumina, titania, aluminophosphates, or combinations thereof [8-13].

* Corresponding Authors - E-mail: ahmadi@znu.ac.ir, z.mohamadnia@iasbs.ac.ir

To make the catalyst, the carrier is impregnated with an aqueous solution of chromium compound such as chromate acetate followed by calcination at high temperatures between 300 and 900 °C in oxygen or dry air to activate the catalyst. In the period of thermal activation, chromium becomes oxidized to Cr(VI), which reacts with surface hydroxyl groups to become anchored and monodispersed [14-16]. This process stabilizes the Cr(VI) against thermal decomposition. The most unique feature of the Phillips catalyst is that the calcined catalyst could be directly activated by ethylene monomer for ethylene polymerization without using organometallic cocatalysts or other reducing agents (such as CO or H_2) [17- 19].

The textural properties of the carrier have a significant effect on the behaviour of Phillips catalysts. So, chromium supported on high pore volume silica presents a higher catalytic activity and therefore produces a lower molecular weight (*MW*) polyethylene with higher melt index (*MI*) [20-22]. Aerogels are highly porous nanostructured materials with low density. They were first reported by Kiestler in the early thirties [23]. These materials possess a number of interesting and unique properties such as high surface area and high porosity that have led to applications in thermal insulation, catalyst supports, acoustics and gas filters [24]. Silica aerogels are generally produced by hydrolysis and condensation of silicon alkoxides such as tetramethyl orthosilicate (TMOS) or tetraethyl orthosilicate (TEOS) in the presence of an acidic or basic catalyst, followed by supercritical drying in an autoclave [25]. Supercritical drying is the very expensive and risky aspect of aerogel making process. A highly desirable goal in aerogel preparation is the elimination of the supercritical drying process which is an important precondition for large-scale application and commercial viability of aerogels. A cheap, simpler, and safer process is obtained by drying at ambient pressure (subcritical drying). However, during drying of a gel under subcritical drying, capillary pressure causes shrinkage of the gel network and cracking frequently occur [26, 27]. This cracking and shrinkage are affected by the gel properties and can be reduced by two important approaches: reducing the capillary tension during drying (solvent exchange) and increasing the strength and stiffness of the wet gel (chemical modification). Although, by combining both approaches, cracking and shrinkage can be even further reduced [28, 29]. However, we decreased the capillary tension by using a liquid with a low surface tension as the pore liquid during subcritical drying without any surface modification. Because of the large contribution of surface modification agents to the total cost, this method seems to be the method of choice for the synthesis of aerogels at an industrial scale [30].

After silica, the most commonly used commercial support is silica–titania. Although titania itself functions poorly as a support for Phillips catalysts, when a few percent titania is added to Cr/silica it serves as a strong promoter for the chromium, increasing its activity and lowering the polymer MW [31, 32].

In the present work, ethylene polymerization was carried out in the slurry phase using Phillips chromium catalyst based on silica materials such as silica aerogel, SiO_2 (G 643) and titanium modified SiO_2 (G 643), and the results were compared with other catalysts based on SiO_2 (Aldrich), SBA-15(Hex), SBA-15(Sp) and MCM-41. In addition, the influence of the support structure on the catalytic activities was investigated.

EXPERIMENTAL

Materials

All manipulations involving air and/or water sensitive compounds were performed under nitrogen atmosphere using standard Schlenk technology. TEA (triethylaluminium), cetyltrimethylammonium bromide (CTABr) and Pluronic 123 triblock copolymer (EO20–PO70–EO20) were purchased from Aldrich. Tetraethylorthosilicate (TEOS), sodium silicate, sulphuric acid, ammonium nitrate, 1-butanol, methanol and ethanol were obtained from Merck. Polymerization-grade ethylene was purified using three columns of KOH, CuO, and 5 °A molecular sieves. Hexane was refluxed over sodium with benzophenone as an indicator and distilled under nitrogen atmosphere before use. Hexagonal SBA-15 (SBA-15(Hex)), Spherical SBA-15 (SBA-15(Sp)) and MCM-41 supports were synthesized according to our previous works [20, 33].

Procedures

Preparation of Silica aerogel

The silica wet gels were prepared using a sodium silicate precursor. The sols were prepared by adding sulphuric acid dropwise to sodium silicate while stirring and the mixtures were kept at 5 °C to form a gel. The formed gels were aged at room temperature

for 48 h under static conditions. The gels were subsequently washed with ammonium nitrate to remove the sodium salt trapped in the pores. Afterwards, solvent exchange was performed with 1-butanol to replace the water in the pores [34]. The wet gels were dried at subcritical pressure by applying heat and vacuum [35, 36]. The final product was calcined at 700°C for 4 h with a heating rate of 5.0 °C min^{-1} under pure nitrogen.

Preparation of the silica supported catalysts

Silica was soxhleted and subsequently outgassed under vacuum overnight. 2.0 g of the silica was stirred with 30 ml of chromium nitrate nonahydrate solution in dried methanol for 3 h under reflux. Next, the solid product was recovered and intensively washed with methanol. Finally, grafted materials were calcined in air at 550 °C for 3 h with a heating rate of 2.0 °C min-1. ICP analysis gave the supported chromium content (0.19 wt %). Different synthesized and commercial types of silica were used as carriers for Cr/silica catalyst preparation.

Preparation of polyethylene in slurry phase

Ethylene polymerization reactions were carried out in a 1 L stainless steel stirred autoclave engineers apparatus using Phillips catalyst based on silica materials such as silica aerogel, SiO_2 (G 643) and titanium modified SiO_2 (G 643), and the results were compared with other catalysts based on SiO_2 (Aldrich), SBA-15(Hex), SBA-15(Sp) and MCM-41. Optimized reaction conditions were 800 rpm, 90 °C,
31.5 bar of ethylene pressure, 0.5 mol of TEA and the use of n-hexane as the solvent. After 1 h of the reaction, the resulting polyethylene (PE) was recovered, filtered, washed with acetone and dried for 6 h at 70 °C. Polymerization activities (kg PE (g Cr)$^{-1}$ h^{-1}) were calculated for each run.

Characterization

Inductively coupled plasma-atomic emission spectroscopy (ICP-AES, 3410, Switzerland) was used to determine the elemental analysis of the synthesized catalysts. Powder X-ray diffraction (XRD) patterns were collected on a Siemens D5000 diffractometer (Siemens, Berlin, Germany) using Cu Kα radiation with a wavelength of 0.154 nm. The FTIR spectra of the samples were recorded using a Perkin- Elmer, 580B instrument in the range of 400 to 4000 cm^{-1} at room temperature from KBr pellets. The thermogravimetric measurements were performed by STA 503 instrument with a heating rate of 10 °C/min in air flow.

The nitrogen adsorption–desorption isotherms were measured on an OMNISORP (TM) 100CX VER 1G adsorption apparatus. The specific surface area of the supports and catalysts was obtained based on the BET (Brunauer, Emmett, and Teller) method. The pore size distribution was calculated using the BJH (Barrett–Joyner–Halenda) method. Differential scanning calorimetry (DSC) analysis was carried out on a Perkin-Elmer (Pyris 1, USA) DSC 7 instrument. Ultrahigh purified nitrogen was purged through the calorimeter. The PE samples (≈4 mg) were heated to 170 °C at a rate of 10 °C min^{-1} followed by cooling to 40 °C at the same rate. Subsequently, a second heating cycle was conducted at a heating rate of 10 °C min^{-1}. The chemical composition of catalysts and supports were measured by EDX method (JEM-35 microscope, JEOL Co., link system ANB-1000, Si–Li detector). High load melt index values of the resultant polymers were obtained using a Ceast 6542/002 extrusion plastometer with a weight load of 21.6 kg at 190 °C. The bulk density of the prepared polyethylene was calculated using the dry weight of a sample and its volume. The volume of the sample was measured in a volumetric tube by liquid displacement.

RESULTS AND DISCUSSION

Characterization of supports and catalysts

Silica aerogel

Figure 1 shows the FTIR spectra of the silica aerogel and Cr/silica aerogel catalyst. The typical Si-O-Si bands around 1070-1220 cm^{-1} associated with the

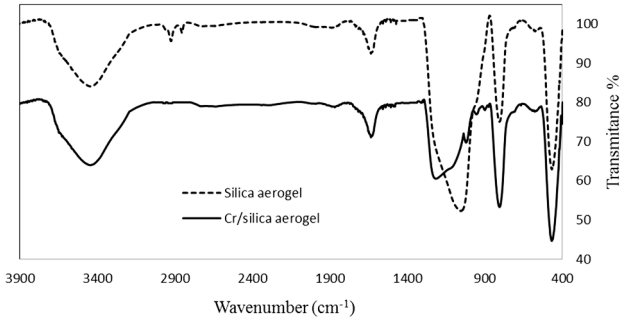

Figure 1. FTIR spectra of silica aerogel and Cr/silica aerogel catalyst.

formation of a condensed silica network are present. The peaks at 1600 cm^{-1} and 3400 cm^{-1} are attributed to the O–H bending and stretching vibration modes. The peaks at 490 cm^{-1} and 800 cm^{-1} are related to the Si-O-Si bending, and symmetric stretching, respectively. The band at 913 cm^{-1}, which is attributed to the Si-O-Cr stretching vibrations of chromium anchored to the surface of silica aerogel support, can be found in the FTIR spectrum of Cr/silica aerogel. This band does not exist in the spectrum of the silica aerogel. These characteristic bands confirm that the chromium is introduced into the silica aerogel.

Nitrogen adsorption–desorption isotherm and the corresponding Barrett–Joyner–Halenda (BJH) pore size distribution curve of the silica aerogel are shown in Figure 2. As shown in Figure 2, the calculated average pore size of the silica aerogel is 16.3 nm. Table 1 summarizes the structural parameters of different supports, including specific surface area, average pore diameter, pore volume, XRD interplanar spacing [37], and pore wall thickness, obtained from the nitrogen adsorption–desorption and XRD analysis. Characterization of the other supports was fully reported in our previous work [20, 33].

Scanning electron microscopy was used to determine the size and morphology of the silica aerogel. The SEM micrographs in Figure 3 show that the silica aerogel particles have a cubic structure with a size of up to 50 μm.

TGA analysis was used to study the thermal stability of the Cr/silica aerogel catalyst. The weight loss of the Cr/silica aerogel at a constant heating rate of 10°C/min under a nitrogen atmosphere is presented in Figure 4. The TGA curve reveals four different regions. Region I shows a sharp decrease in the weight as the sample is heated up from room temperature to almost 100 °C. In this region the weight of the sample decreases by about 2.5%, which can be attributed to the evaporation of the methanol residues. Region II lies between 100 and 250 °C and is associated with a small weight loss of about 0.5% which can be attributed to the evaporation of physically absorbed water. Region III falls between 250 and 800 °C and reveals a weight loss of approximately 2%, which can be related to the evaporation of the water formed through conversion of hydroxyl groups of the support

Table 1. Structural parameters of synthesized and commercial samples.

Sample	Support	S_{BET} $m^2\ g^{-1}$	d_p Å	V_p $ml\ g^{-1}$	d_{100} Å	b_p Å
1	SiO_2 (Aldrich)	500	60	0.75	74	12.7
2	SiO_2 (Grace 643)	300	150	1.15	-	-
3	Silica aerogel	302	163	1.32	-	-
4	SBA-15 (Hex)	479	35.8	0.51	87	32.4
5	MCM-41	583.6	12.9	0.28	41	17.2
6	SBA-15 (Sp)	894.5	106	3.6	103	6.5

S_{BET}, BET specific surface area; V_p, specific pore volume; d_p, average pore diameter, obtained from BJH adsorption data, $d_p = 4V_p/S_{BET}$; d_{100}, XRD interplanar spacing; bp, pore wall thickness, $b_p = (a_0 - d_p)/2$, $a_0 = (2\sqrt{3})d_{100}$.

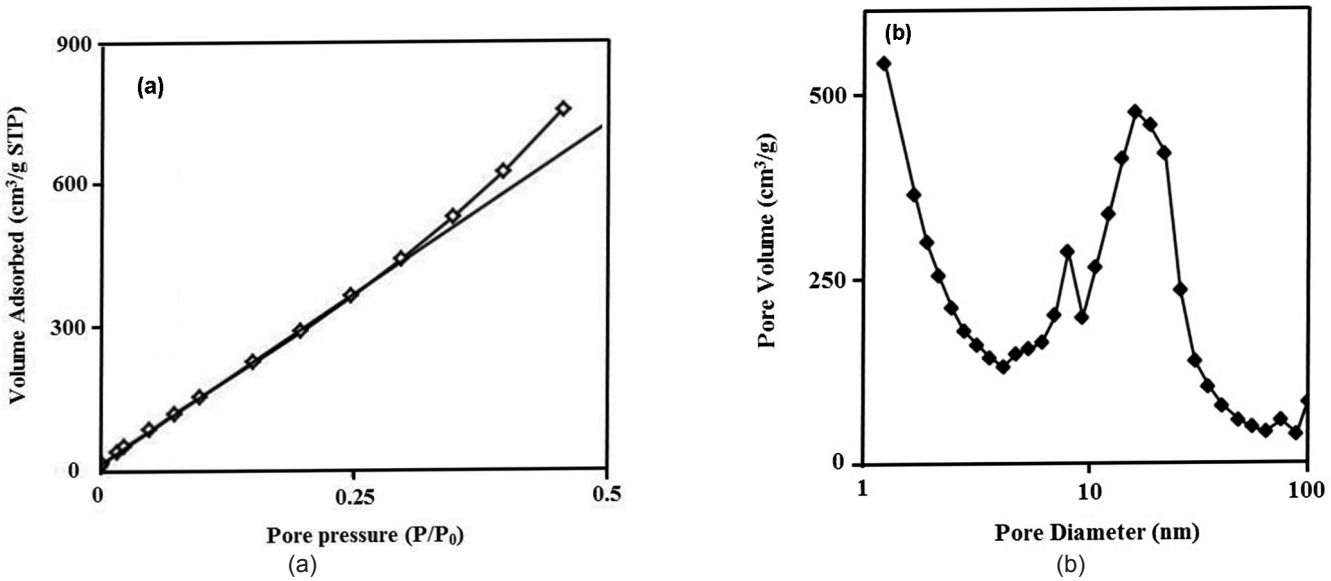

(a) (b)

Figure 2. (a) Nitrogen adsorption-desorption isotherm plot and (b) Pore size distribution curve of silica aerogel.

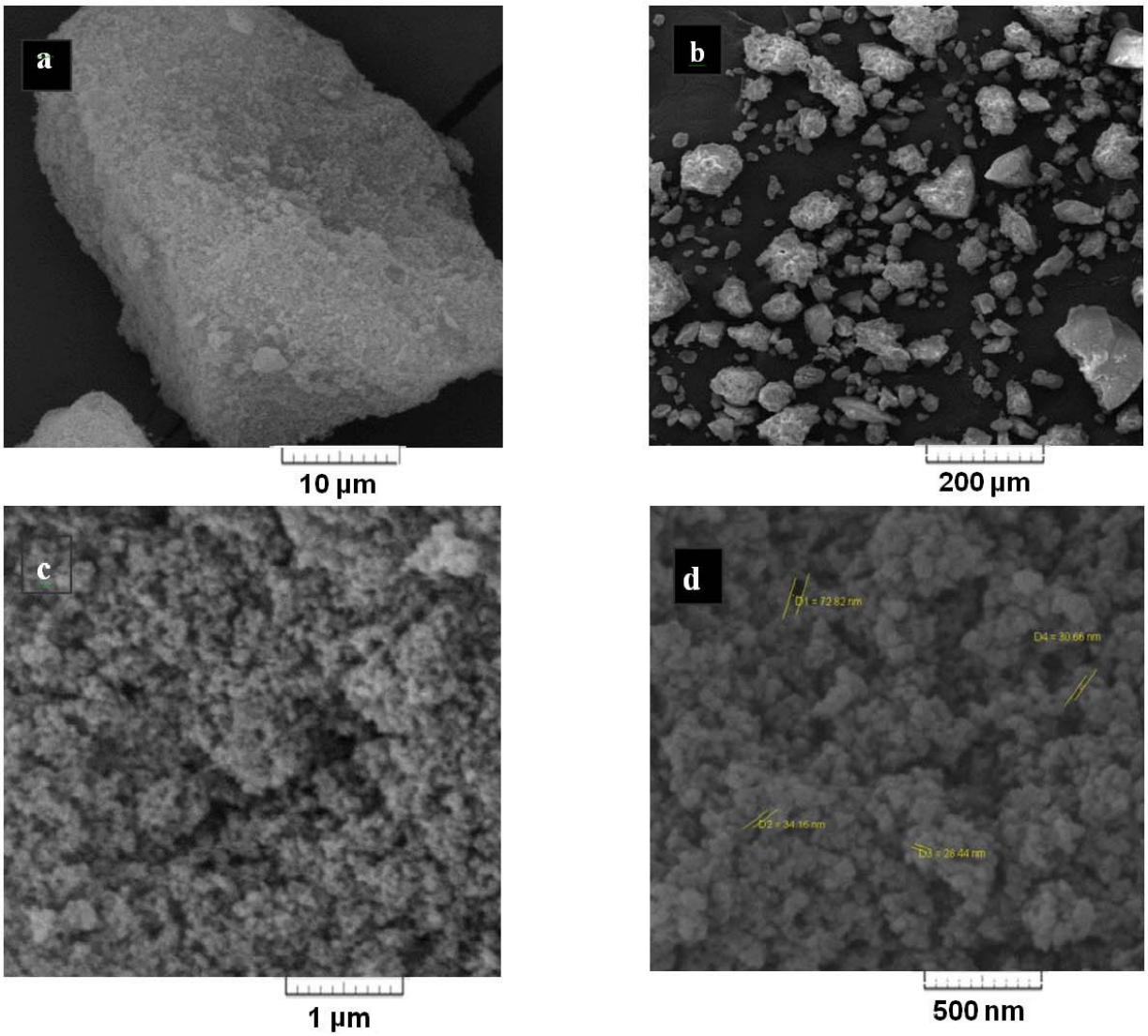

Figure 3. SEM images of silica aerogel (a) 10 µm, (b) 200 µm, (c) 1 µm, (d) 500 nm.

surface to epoxy. Finally, Region IV lies between 800 and 1200 °C, which shows a weight loss of around 6% due to sintering of the silica structure. As a result, a total weight loss of approximately 11% was reached on heating from the room temperature up to 1200 °C.

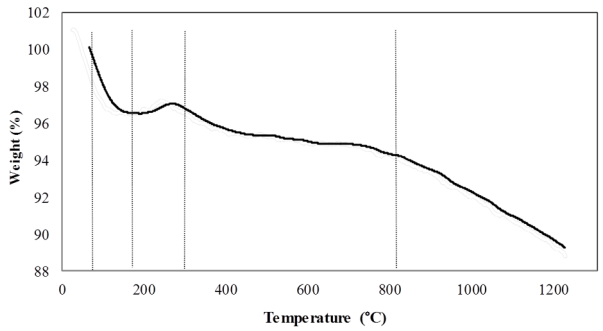

Figure 4. Weight loss of Cr/silica aerogel heated at 10 °C/min in nitrogen as measured by TGA.

The SEM micrographs in Figure 5 show that the Cr/silica aerogel catalyst has the same structure as the silica aerogel. Moreover, in comparison with the silica particles the geometry has not changed a lot and still retains a cubic form. However, some little surface wear due to repeated calcination is seen.

Grace silica (G 643)

Figure 6 displays the infrared (IR) spectra (KBr technique) of the SiO_2 (G 643) and Cr/SiO_2 (G 643) catalysts. It may be noted that SiO_2 (G 643) shows a small band near to 970 cm^{-1}, which is the characteristic of silanol groups in the mesoporous material. Upon addition and grafting of chromium a small shift of about 10 cm^{-1} to lower frequencies and a slight broadening of this band could be detected. This can be reasonably because of the modification

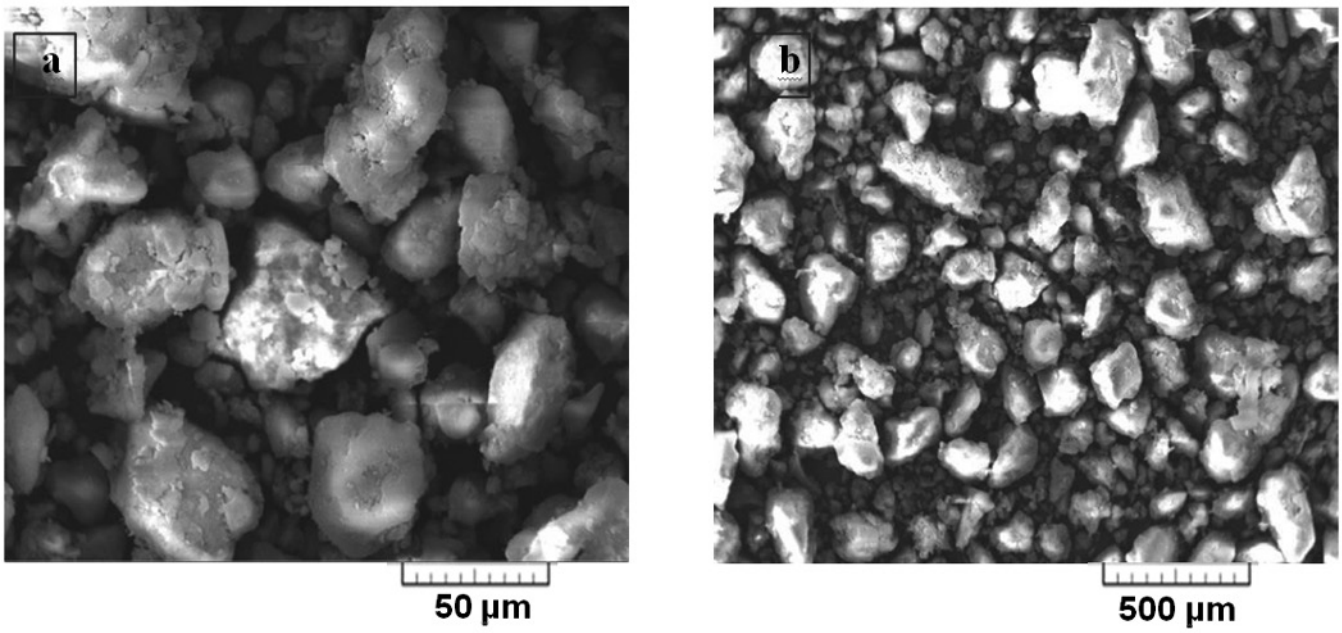

Figure 5. SEM micrographs of Cr/silica aerogel (a) 50 µm, (b) 500 µm.

in the silanol strength due to the presence of a near lying Cr atom (–Si–O–Cr). As shown in Figure 6, the broad band between 1070-1220 cm^{-1} is due to the symmetrical stretching vibration of Si-O-Si that reveals the structural stability of chromium atoms and Grace silica during the reaction.

Figure 7 shows the nitrogen adsorption–desorption isotherm of the Grace silica. Table 1 summarizes the textural properties of the Grace silica support derived from nitrogen adsorption-desorption isotherm plot and pore size distribution curve.

From the SEM observations, the Cr/Grace SiO_2 catalyst consists of particles that are 10 to 70 µm in diameter (see Figure 8).

Ethylene polymerization results

Table 2 summarizes both catalyst activities and properties of the obtained polymers. The activity of Cr/SiO_2(G 643) is 191 kg PE (g Cr)$^{-1}$ h^{-1} which is almost 6 times higher than that of the other catalysts. This is due to the high pore diameter (150 °A) and

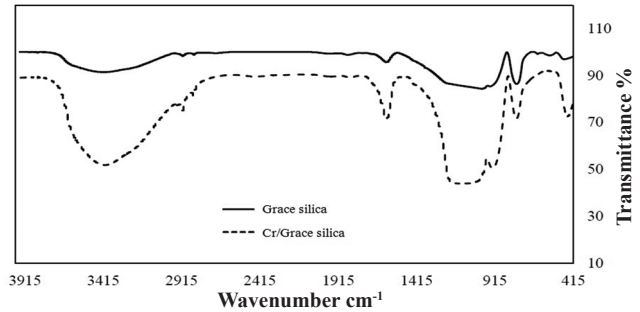

Figure 6. FTIR spectra of the Grace silica support and Cr/Grace silica catalyst.

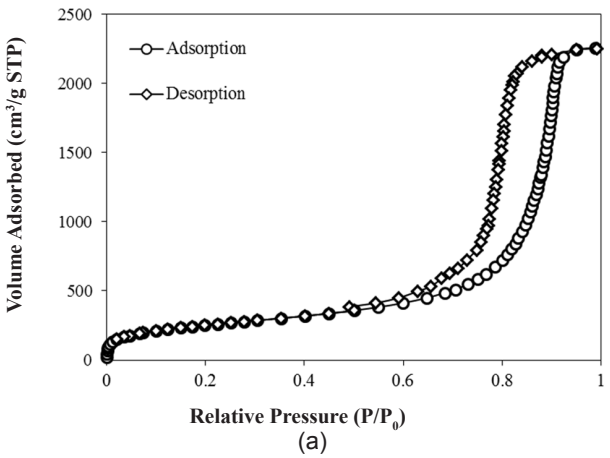

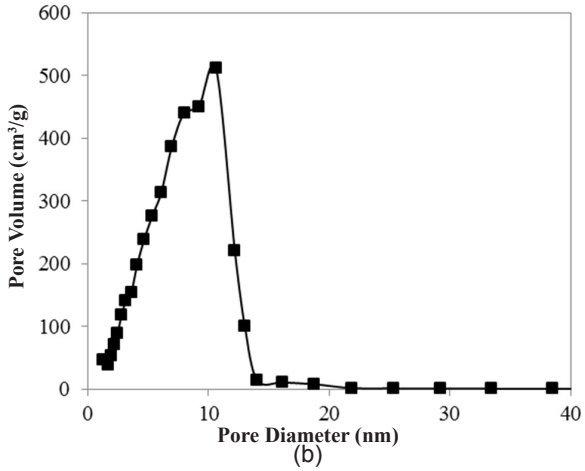

Figure 7. (a) Nitrogen adsorption-desorption isotherm plot and (b) Pore size distribution curve of Grace silica.

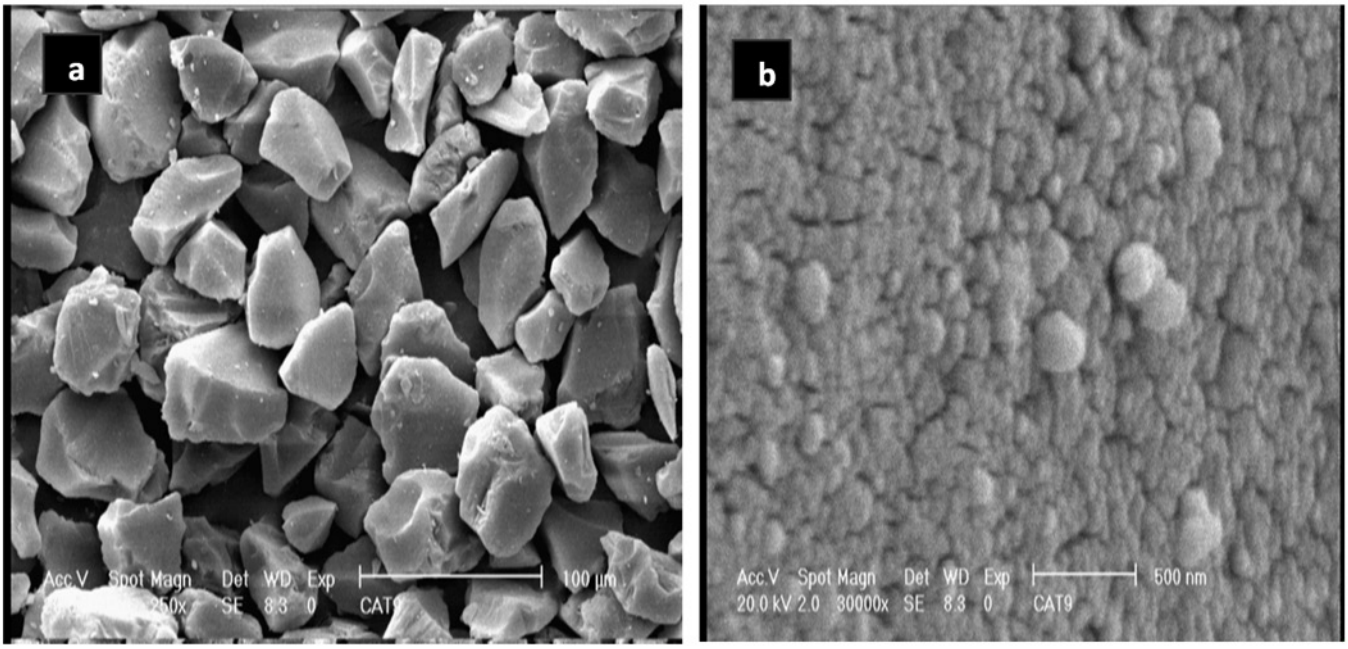

Figure 8. SEM micrographs of catalysts (a) Cr/SiO_2 (G 643) (b) magnified view of (a).

high pore volume (1.15 ml g^{-1}) of SiO_2(G 643) support (Table 1). As shown in Table 2, catalysts number 2 and 6 show approximately the same activity, because the SiO_2 (G 643) support has small pore volume and large pore diameter while SBA-15(Sp) has large pore volume and high specific surface area. Bulk density of the polymer produced by the Cr/SiO_2(G 643) catalyst is almost twice as much as that produced by the other catalysts (Table 2).

The high activity of Cr/SBA-15(Sp) (175 kg PE (g Cr)$^{-1}$ h^{-1}) is related to the high specific surface area (894.5 m^2 g^{-1}) and high pore volume (3.6 ml g^{-1}) of SBA-15(Sp) (Table 1).

The activity of Cr/SBA-15(Hex) is higher than that of Cr/SiO_2(Ald). The Cr/SBA-15(Hex) catalyst prepared by impregnation, produced polyethylene with slightly higher melting temperature in comparison to the polyethylene obtained from the Cr/SiO_2(Ald) catalyst. This indicates that the channels of SBA-15(Hex) can control the direction of the chain propagation to increase the crystallinity of the polyethylene [38].

It is remarkable that the Cr/SBA-15(Hex) catalyst showed a very low catalytic activity in spite of the high surface area of its support. The probable explanation is that the just formed polymer fills up the pores of the material immediately. On the other hand, the catalyst structure is not fragile enough to fragment into smaller pieces. Consequently, the material cannot produce further polymer. Fragility is often correlated with pore volume. Thus, the Cr/silica catalysts with much less than 1.0 cm^3 g^{-1} pore volume and 100 °A pore size, usually do not exhibit polymerization activity [34]. In this way, the small pore size, small pore volume, and high wall thickness of SBA-15(Hex) support (Table

Table 2. Ethylene polymerization results with synthetic and commercial silica chromium supported catalysts[(a)].

Run[(a)]	Catalysts	Activity (kg PE (gCr)$^{-1}$ h^{-1})	Bulk density (gml $^{-1}$)	T[(b)] First scan (°C)	T[(b)] Second scan (°C)	ΔH First scan (J g^{-1})	ΔH Second scan (J g^{-1})	Crystallinity[(c)]
1	Cr-SiO_2(Aldrich)	13.4	0.21	138.9	135.2	170.4	150.4	58.0
2	Cr/SiO_2(G 643)	191	0.43	133.8	133.4	213.6	213.2	72.7
3	$Cr/Ti/SiO_2$(G 643)	380	0.44	133.3	132.6	209.8	211.8	71.5
4	Cr/Silica aerogel	-	0.44	138	-	228	-	77.8
5	Cr/MCM-41	15	0.2	141.4	136.5	204.8	162.7	69.8
6	Cr/SBA-15(Sp)	175	0.26	141.6	135.9	198.7	164.4	67.7
7	Cr-SBA-15(Hex)	34	0.15	142.8	137.0	207.8	163.6	70.7

(a) Polyethylene pressure=31.5 bar; solvent=n-hexane; cocatalyst=TEA, Tp (polymerization temperature)=90 °C; (b) Melting temperature measured by DSC; (c) Crystallinity measured by XRD.

1) are responsible for the low polymerization activity of the Cr/SBA-15(Hex) catalyst compared to the other catalysts.

The high activity of Cr/SiO_2(G 643) catalyst is attributed to its chemical composition. According to EDX elemental analysis, there is a small amount of titanium (Ti/SiO_2=0.07 wt%) in the SiO_2(G 643) support. The presence of titania enhances the Brönsted acidity of the surface, and the chromium may associate with or link to these strongly acidic Brönsted sites. This bonding would tend to make the chromium more electron deficient and more likely to react with olefins [31, 39]. The increase in the surface acidity may derive from an ability of Ti(IV) to assume a tetrahedral coordination and fit in the silica lattice [40].

To confirm the above results, Cr/Ti/SiO_2 (G 643) catalyst was prepared by grafting titanium tetraisopropoxide $(Ti\text{-}OPri)_4$ onto the SiO_2 (G 643) (Ti/Si=0.8 wt%) surface in an N_2 atmosphere. According to Table 2 run 3, the activity significantly increases with titanium incorporation. These effects are perhaps caused by Cr(VI) ions attached to Brönsted acid sites, which possibly pull electron density away from the chromium, making it more Lewis acidic.

These facts could be explained by taking into account that the wall thickness of SiO_2 (G 643) and Ti/SiO_2 (G 643) samples are reduced by Ti incorporation, resulting at the same time in higher pore volumes (Table 1). High pore volume, pore size, and small wall thickness of modified supports are responsible for high polymerization activity exhibited by the Cr/SiO_2 (G 643) and Cr/Ti/SiO_2 (G 643) catalysts. These two circumstances lead to materials that are more fragile and consequently more active in ethylene polymerization.

DSC analysis was used for the thermal characterization of the PE produced by the Cr/silica aerogel (Figure 9). The DSC curve shows an exothermic peak at 138 °C (ΔH = 228 J/g), whereas the melting point of the melt-crystallized high-density polyethylene is in the range of 133 to 135 °C. This may be attributed to the high molecular weight polymer chains having a small number of side branches, which result in extended-chain crystals.

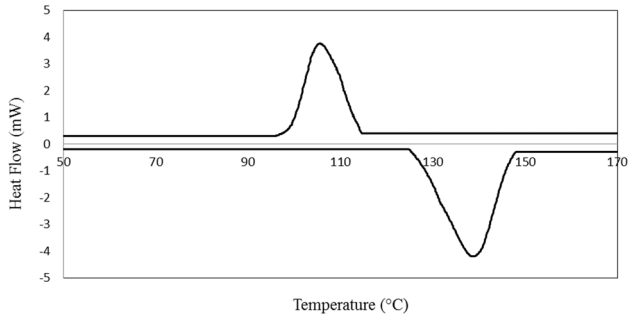

Figure 9. DSC thermogram of polyethylene produced by Cr/silica aerogel.

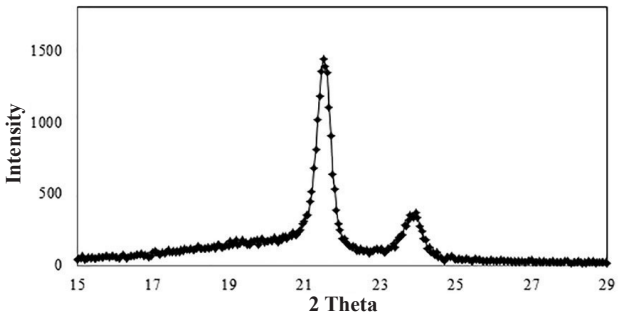

Figure 10. XRD spectra of polyethylene sample prepared using silica aerogel-supported catalyst.

The DSC results show that the melting point of the polymer prepared with the Cr/SiO_2 (G 643) catalyst (133.8°C) is similar to that prepared with the Cr/Ti/SiO_2 (G 643) catalyst (133.3°C). According to these analysis, the first and second scans were identical. Therefore, the crystalline structure of the polymer is independent of its thermal history and the structure of the polymer produced by Cr/SiO_2 (G 643) and Cr/Ti/SiO_2 (G 643) is preserved.

Figure 10 shows the main peaks of the XRD pattern of the polyethylene prepared using the Cr/silica aerogel catalyst. The peaks [110] and [200] at 21.5° and 23.9°, respectively correspond to the crystalline structure of polyethylene, while a small amorphous halo around 19.50° corresponds to the existence of amorphous polyethylene. Also, the typical orthorhombic crystal structure for the crystalline polyethylene prepared with Cr/SiO_2 (G 643) and Cr/Ti/SiO_2 (G 643) was consistent with two peaks indexed at 21.9° and 24.3° in the XRD pattern shown in Figure 11. The additional halo around 19.50° indicating the existence of floccules [41]. The results show that the polyethylene prepared using the Cr/silica aerogel catalyst has the highest crystallinity among the other polyethylene samples. The different degrees of crystallinity may be attributed to the differeces in structures of silica supported catalysts which is consistent with the DSC results, as shown in Table 2.

Figure 12 shows the SEM micrographs of the polyethylene produced by the Cr/silica aerogel, which indicate the sample has mainly porous morphology. In

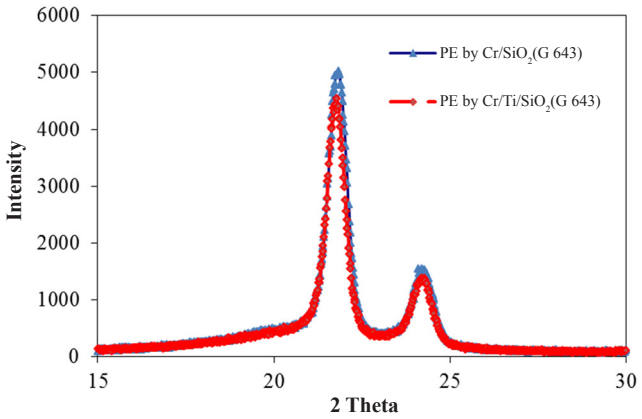

Figure 11. XRD spectra of polyethylene samples prepared with silica-supported catalysts.

addition, it shows that each catalyst particle produces a polymer particle of approximately the same shape as the catalyst particle, but several times larger.

The SEM micrographs of the sample produced in Table 2 run 3 show that the polymer has taken a shish-kebab morphology (Figures 13 and 14). The shish-kebab morphology in these figures reveals the high crystallinity of the PE produced by Cr/SiO_2 (G 643) and $Cr/Ti/SiO_2$ (G 643) [42]. According to Pennings [43] the shish-kebab structure consists of a central filament or backbone which is covered with platelets at rather regular intervals. After the discovery of this structure by Pennings et al. many reports on the shish- kebab structure of polymers, crystallized from solutions [44, 45] and also melts [46, 47], have been reported.

CONCLUSION

Silica aerogel was synthesized and studied as a support for Phillips chromium catalyst. Ethylene polymerization was carried out in the slurry phase using Phillips catalyst based on silica materials such as silica aerogel, SiO_2 (G 643), and titanium modified SiO_2 (G 643), and the results were compared with other catalysts based on SiO_2 (Aldrich), SBA-15(Hex), SBA-15(Sp) and MCM-41. The materials were characterized with thermogravimetrical analysis (TGA), differential scanning calorimeter (DSC), X-ray diffraction (XRD), nitrogen adsorption–desorption, scanning electron microscopy (SEM), inductively coupled plasma (ICP) and Fourier transform infrared spectroscopy (FTIR). The results showed that the chromium was successfully introduced into the silica aerogel. Moreover, the bulk density, melting temperature and crystallinity of the obtained polymers were comparable to those of high-density polyethylene.

Shish-kebab polyethylene was prepared via in situ ethylene polymerization with the Grace silica-supported chromium nitrate nonahydrate catalytic systems. We could show the Shish-kebab structure was the major morphological unit in the samples.

This work showed that the effect of titanium on the Phillips catalyst activity is more powerful than other structural parameters. Titanium atoms on the support walls decrease the electron density and finally increase the activity.

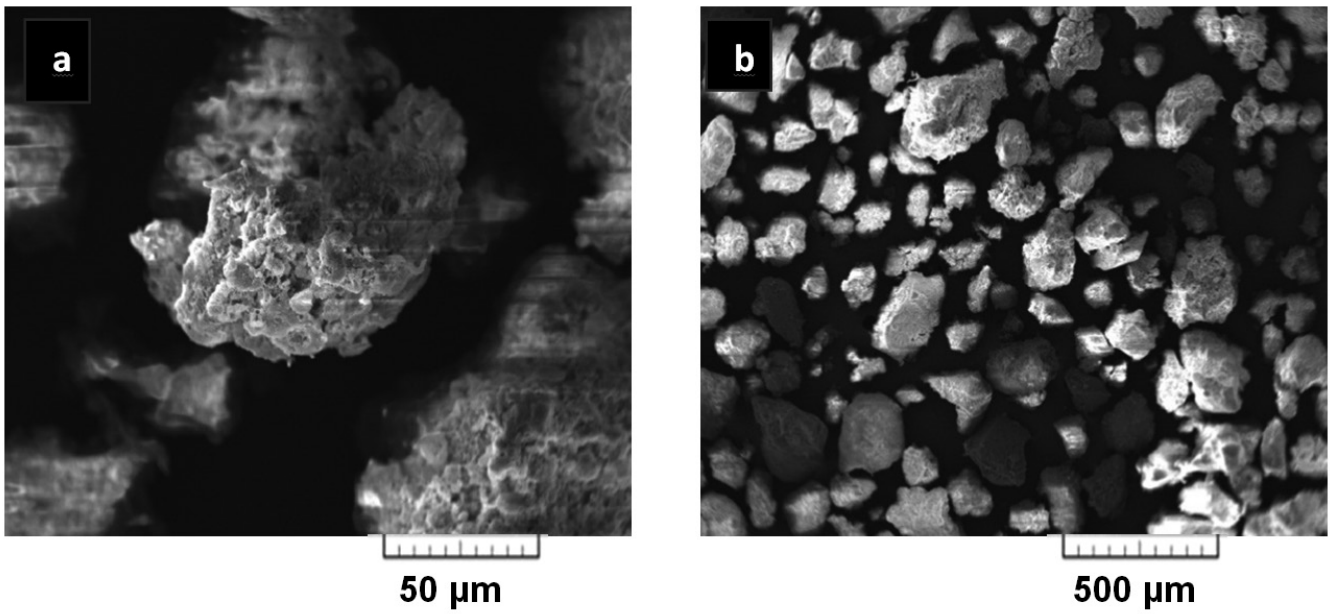

Figure 12. SEM micrographs of polyethylene produced from Cr/silica aerogel (a) 50 µm, (b) 500 µm.

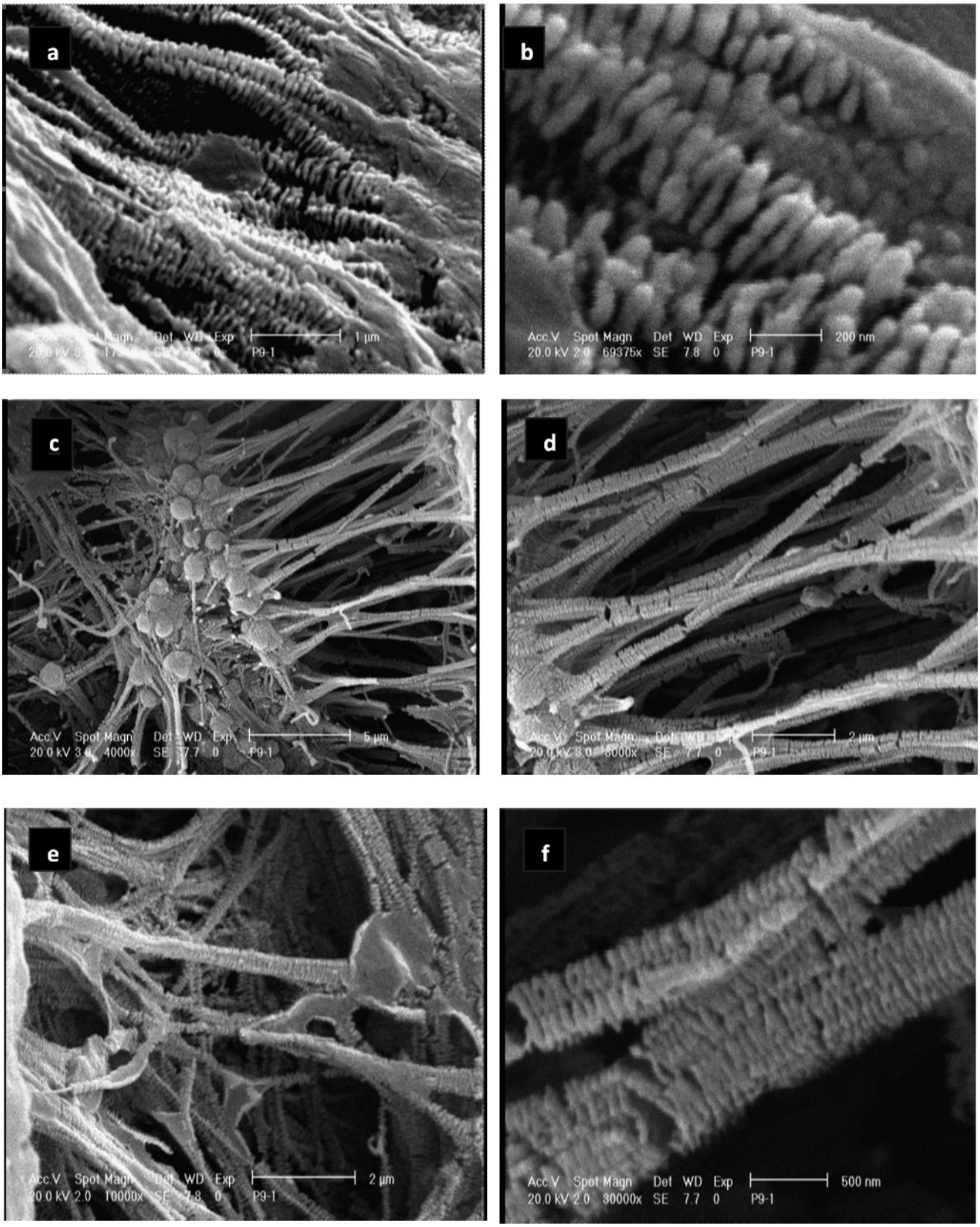

Figure 13. SEM micrographs of the polyethylene produced from chromium supported catalysts at 90 °C polymerization (a) Cr/SiO_2(G 643) (magnification ×17000), (b) (magnification×69375), (c) another view of Cr/SiO_2(G 643) (magnification ×4000), (d) (magnification ×8000), (e) (magnification ×10000) and (f) (magnification ×30000).

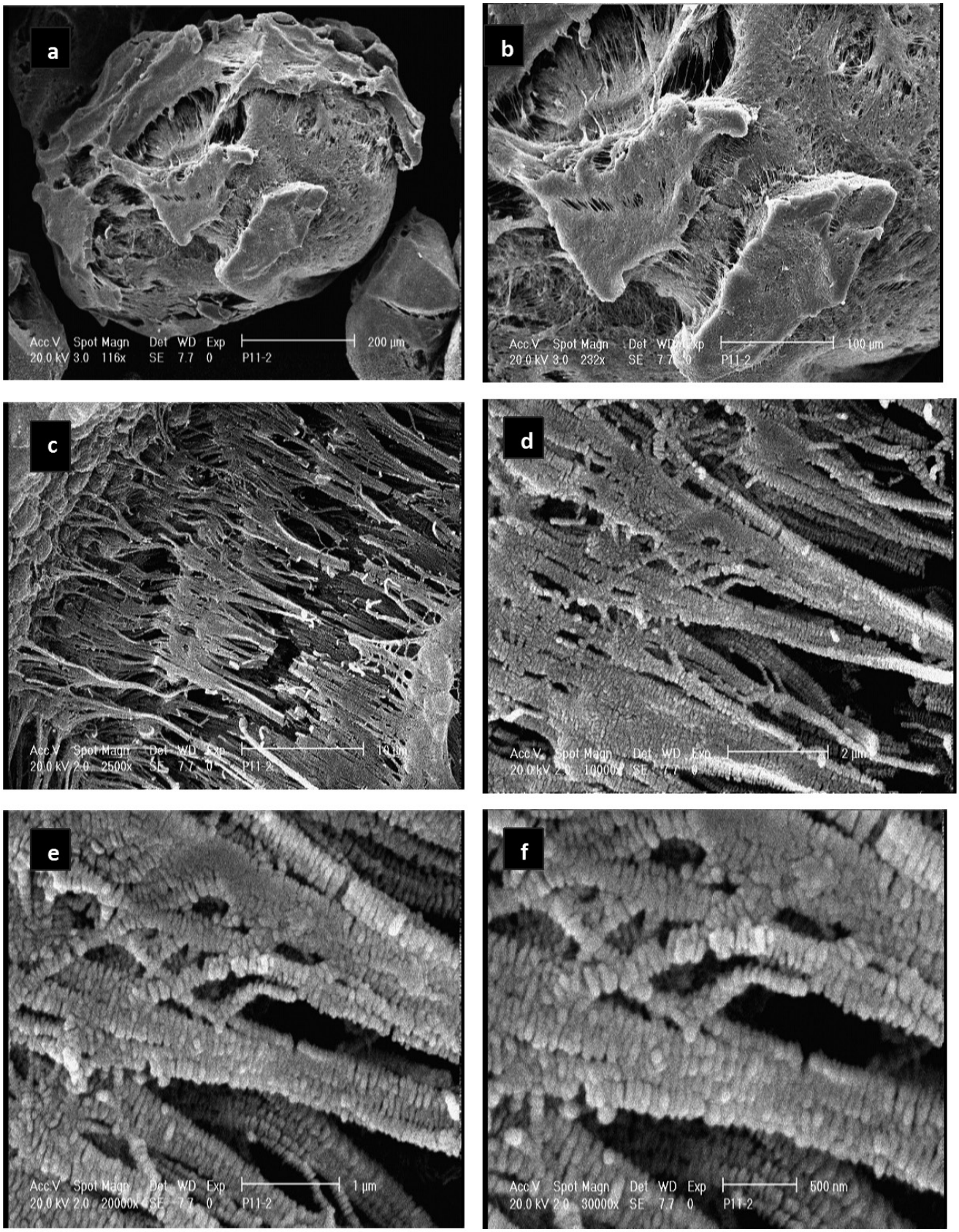

Figure 14. SEM micrographs of the polyethylene produced from chromium supported catalysts at 90 °C polymerization (a) Cr/Ti/SiO_2(G 643) (magnification×116) (b) (magnification ×232), (c) (magnification ×2500), (d) (magnification ×10000), (e) (magnification ×20000) and (f) (magnification ×30000).

REFERENCES

1. McDaniel MP (1985) Supported chromium catalysts for ethylene polymerization. Adv Catal 33: 47-98
2. Weckhuysen BM, Schoonheydt RA (1999) Polymerization over supported chromium oxide catalysts. Catal Today 51: 215-221
3. McDaniel MP (2010) Chapter 3 - A review of the Phillips supported chromium catalyst and its commercial use for ethylene polymerization. Adv Catal 53: 123-606
4. Zhang J, Qiu P, Liu Z, Liu B, Batrice RJ, Botoshansky M, Eisen MS (2015) Mechanistic studies on the switching from ethylene polymerization to nonselective oligomerization over the triphenylsiloxy chromium(II)/ methylaluminoxane catalyst. ACS Catalysis 5: 3562-3574
5. Groppo E, Lamberti C, Bordiga S, Spoto G, Zecchina A (2005) The structure of active centers and the ethylene polymerization mechanism on the Cr/SiO_2 catalyst: A frontier for the characterization methods. Chem Rev 105: 115-183
6. Tonosaki K, Taniike T, Terano M (2011) Origin of broad molecular weight distribution of polyethylene produced by Phillips-type silica-supported chromium catalyst. J Mol Catal A: Chem 340: 33–38
7. Cheng R, Liu Z, Zhong L, He X, Qiu P, Terano M, Eisen MS, Scott SL, Liu B (2013) Phillips Cr/ silica catalyst for ethylene polymerization. Adv Poly Sci 257: 135-202
8. McDaniel MP (2008) Review of Phillips chromium catalyst for ethylene polymerization. In: Handbook of heterogeneous catalysis, Wiley-VCH, Weinheim, 3733-3792
9. Ma Y, Wang L, Liu Z, Cheng R, Zhong L,Yang Y, He X, Fang Y, Terano M, Liu B (2015) High-resolution XPS and DFT investigations into Al-modified Phillips $CrOx/SiO_2$ catalysts. J Mol Catal A: Chem 401: 1–12
10. Aguado J, Calleja G, Carrero A, Moreno J (2010) Morphological modifications of Cr/SBA-15 and Cr/Al-SBA-15 ethylene polymerization catalysts: Influence on catalytic behaviour and polymer properties, Micropor Mesopor Mater 131: 294–302
11. Ma Y, Cheng R, Li J, Zhong L, Liu Z, He X, Liu B (2015) Effect of Mo-modification over phillips $CrOx/SiO_2$ catalyst for ethylene polymerization. J Organomet Chem 791: 311-321
12. Matta A, Zeng Y, Taniike T, Terano M (2012) Vanadium-modified bimetallic Phillips catalyst with high branching ability for ethylene polymerization. Macromol React Eng 6: 346–350
13. Cheng R, Xue X, Liu W, Zhao N, He X, Liu Z, Liu B (2015) Novel SiO_2-supported chromium oxide(Cr)/vanadium oxide(V) bimetallic catalysts for production of bimodal polyethylene. Macromol React Eng doi: 10.1002/mren.201400072
14. Conley MP, Delley F, Núñez-Zarur F, Comas-Vives A, Copéret C (2015) Heterolytic activation of C−H bonds on Cr^{III}−O surface sites is a key step in catalytic polymerization of ethylene and dehydrogenation of propane. Inorg Chem 54: 5065–5078
15. Zecchina A, Groppo E, Damin A, Prestipino C (2005) Anatomy of catalytic centers in Phillips ethylene polymerization catalyst. Top Organomet Chem 16: 1–35
16. Chakrabarti A, Wachs IE (2015) The nature of surface CrO_x sites on SiO_2 in different environments. Catal Lett 145: 985–994
17. McDaniel MP, Schwerdtfeger ED, Jensen D (2014) The "comonomer effect" on chromium polymerization catalysts. J Catal 314: 109–116
18. Zhao N, Cheng R, Dong Q, He X, Liu Z, Zhang S, Terano M, Liu B (2014) Tuning the short chain branch distribution of ethylene and 1-hexene copolymers by SiO_2-supported silyl chromate catalyst with different Al-alkyl co-catalysts. Polyolefins J 1: 93-105
19. Fong A, Yuan Y, Ivry SL, Scott SL, Peters B (2015) Computational kinetic discrimination of ethylene polymerization mechanisms for the Phillips (Cr/SiO_2) catalyst. ACS Catalysis 5: 3360-3374
20. Mohamadnia Z, Ahmadi E, Nekoomanesh M, Ramazani A, Salehi-Mobarakeh H (2010) Effect of support structure on activity of Cr/ nanosilica Catalysts and morphology of prepared polyethylene. Polym Int 59: 945-953
21. Budnyk A, Damin A, Groppo E, Zecchina A, Bordiga S (2015) Effect of surface hydroxylation on the catalytic activity of a $Cr(II)/SiO_2$ model system of Phillips catalyst. J Catal 324: 79–87
22. McDaniel M P (2011) Influence of catalyst porosity on ethylene polymerization. ACS Catal

1:1394-1407
23. Kistler SS (1931) Coherent expanded aerogels and jellies. Nature 127:741-741
24. Pierre A C, Pajonk G M (2002) Chemistry of aerogels and their applications. Chem Rev 102: 4243- 4266
25. Rao AV, Pajonk GM, Bangi UKH, Rao AP, Koebel MM (2011) Sodium silicate based aerogels via ambient pressure drying. In: Aerogels handbook, Springer, New York, 103-124
26. Haereid S, Nilsen E, Einarsrud M-A (1996) Subcritical Drying of Silica Gels. J Porous Mater 2: 315-324
27. Liu H, Sha W, Cooper AT, FanM (2009) Preparation and characterization of a novel silica aerogel as adsorbent for toxic organic compounds. Colloids and Surfaces A: Physicochem Eng Aspects 347: 38–44
28. Burger T, Fricke J (1998) Aerogels: Production, modification and applications. Berichte der Bunsengesellschaft für physikalische Chemie 102: 1523–1528
29. Zong S, Wei W, Jiang Z, Yan Z, Zhua J, Xie J (2015) Characterization and comparison of uniform hydrophilic/hydrophobic transparent silica aerogel beads: Skeleton strength and surface modification. RSC Adv 5: 55579-55587
30. Sarawade PB, Kim J-K, Hilonga A, Quang DV, Jeon SJ, Kim HT (2011) Synthesis of sodium silicate-based hydrophilic silica aerogel beads with superior properties: Effect of heat-treatment. J Non-Crystal 357: 2156–2162
31. Ahmadi E, Mohamadnia Z, Mashhadi-Malekzadeh A, Hamdi Z, Saghatchi F (2013) Preparation, characterization, and polymerization of chromium complexes-grafted Al/SBA-15 and Ti/SBA-15 nanosupports. J Appl Polym Sci 128: 4245–4252
32. Cheng R, Xu C, Liu Z, Dong Q, He X, Fang Y, Terano M, Hu Y, Pullukat TJ, Liu B (2010) High- resolution spectroscopy (XPS, 1H MAS solid-state NMR) and DFT investigations into Ti-modified Phillips CrO_x/SiO_2 catalysts. J Catal 273: 103–115
33. Ahmadi E, Nekoomanesh Haghighi M, Mohamadnia Z, Ramazani A (2010) Preparation of shish-kebab and nanofiber polyethylene with chromium/Santa Barbara amorphous silica-15 catalysts. J Appl Polym Sci 118: 3658-3665
34. McDaniel M P (2010) Review of Phillips chromium catalyst for ethylene polymerization. In: Handbook of transition metal polymerization catalysts, Wiley-VCH, New Jersey, 291-446
35. Wang Z, Dai Z, Wu J, Zhao N, Xu J (2013) Vacuum-dried robust bridged silsesquioxane aerogels. Adv Mater 25: 4494-4497
36. Zapata PMC, Nazzarro MS, Gonzo EE, Parentis ML, Bonini NA (2015) Cr/SiO_2 mesoporous catalysts: Effect of hydrothermal treatment and calcination temperature on the structure and catalytic activity in the gas phase dehydration and dehydrogenation of cyclohexanol. Catal Today doi:10.1016/j.cattod.2015.04.038
37. Fultz B, Howe J (2013) Transmission electron microscopy and diffractometry of materials. 4th ed., Springer, 1-57
38. Kageyama K, Tamazawa J, Aida T (1999) Extrusion polymerization: Catalyzed synthesis of crystalline linear polyethylene nanofibers within a mesoporous silica. Science 285: 2113-2115
39. Ellison A, Overton TL (1993) Characterisation of Cr/silica catalysts. Part 2.—Ti- and Mg-modified catalysts. J Chem Soc Faraday Trans 89: 4393-4395
40. Soult AS, Carter DF, Schreiber HD, Van de Burgt LJ, Stiegman AE (2002) Spectroscopy of morphous and crystalline titania−silica materials. J hys Chem B 106: 9266-9273
41. Krimm S, Toblosky AV (1951) Quantitative X-ray studies of order in amorphous and crystalline polymers. Quantitative X-ray determination of crystallinity in polyethylene. J Polym Sci 7: 57-76
42. Kimata S, Sakurai T, Nozue Y, Kasahara T, Yamaguchi N, Karino T, Shibayama M, Kornfield JA (2007) Molecular basis of the shish-kebab morphology in polymer crystallization. Science 316: 1014-1017
43. Pennings AJ (1980) Polymer crystallization. J Cryst Growth 48: 574-581
44. Krueger D, Yeh GSY (1972) Morphology of polyethylene microfibrils and “shish kebabs”. J Macromol Sci: Phys 6: 431-450
45. Nagasawa T, Shimomura Y (1974) Mechanism of formation of shish kebab structures. J Polym Sci 12: 2291-2308
46. Hobbs JK, Humphris ADL, Miles MJ (2001) In-Situ Atomic Force Microscopy of Polyethylene Crystallization. 1. Crystallization from an Oriented Backbone. Macromolecules 34: 5508-5519

47. Liu T, Tjiu W C, Petermann J (2002) Transmission electron microscopy observations on fine structures of shish-kebab crystals of isotactic polystyrene by partial melting. J Cryst Growth 243: 218-223